

1 Article

2 Structural Evolution of Two-phase Blends of 3 Polycarbonate and PMMA by Simultaneous Biaxial 4 Stretching

5 Takumi Kobayashi¹ and Hiromu Saito^{1*}

6 ¹ Department of Organic and Polymer Materials Chemistry; Tokyo University of Agriculture and
7 Technology; Koganei-shi, Tokyo 184-8588; Japan

8 * Correspondence: hsaitou@cc.tuat.ac.jp

9
10

11 **Abstract:** We investigated the structural evolution of the two-phase blends of polycarbonate (PC)
12 and poly(methyl methacrylate) (PMMA) at various blend compositions by simultaneous
13 biaxial stretching using optical microscopy and SEM observation. The spherical PMMA domains
14 and PC matrix in 30/70 PC/PMMA were enlarged uniformly at all in-plane direction, while the
15 anisotropic-shaped co-continuous structure in 50/50 PC/PMMA was deformed to crosshatched one
16 by in-plane bimodal orientation. In 70/30 PC/PMMA, the phase inversion was found to occur by
17 simultaneous biaxial stretching; i.e., the spherical PMMA domains were changed to
18 crosshatched matrix by in-plane bimodal orientation due to coalescence of the PMMA domains
19 during the stretching. Owing to the phase inversion, the surface hardness estimated by pencil
20 hardness test became harder from 2B to 2H with increasing the strain from 1.0 to 2.0.

21 **Keywords:** Biaxial stretching; blend; polycarbonate; PMMA; phase inversion; surface hardness

22

23 1. Introduction

24 Biaxially stretched polymer films are often used as packaging materials for food and industrial
25 products because the mechanical and gas barrier properties can be improved by biaxial stretching in
26 the manufacturing process [1]. The structure of polymer films obtained by biaxial stretching are
27 investigated in various aspects [2-34]. Isotropic plane film can be produced by simultaneous biaxial
28 stretching in which films are stretched to X and Y directions at the same time, so that the properties
29 of the stretched specimen thus produced are isotropic in the in-plane direction [19,29,31]. This
30 indicates that uniform orientation at all in-plane direction is caused by simultaneous biaxial
31 stretching; i.e., polymer chains and crystalline lamellae are uniformly oriented at all in-plane
32 direction. The *in-situ* polarized infrared spectroscopic study by Nitta et al. suggests that molecular
33 chain is elongated uniformly at all in-plane direction by simultaneous biaxial stretching of isotropic
34 polypropylene [24,33]. Though the uniform orientation without preferred orientation is considered
35 in the simultaneous biaxial stretching, bimodal orientation to the stretching directions of X and Y is
36 also suggested by wide angle x-ray diffraction study in crystalline polymers such as polyethylene
37 terephthalate (PET) and polyethylene naphthalate [4,29]. However, it is difficult to clarify the bimodal
38 orientation of the structure in neat polymers because of the difficulty for the observation of the
39 stretched structure.

40 In this paper, to observe the stretched structure obtained by simultaneous biaxial stretching, we
41 investigated the evolution of the two-phase structure of polymer blends by simultaneous biaxial

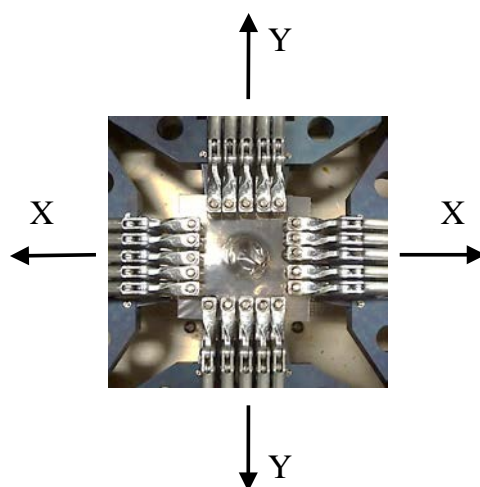
42 stretching using optical microscopy and SEM observation. When the two-phase structure obtained
43 after simultaneous stretching is isotropic, it is considered that the domain structure is enlarged
44 uniformly at all in-plane direction, for instance. We chose the blends of bisphenol-A-polycarbonate
45 (PC) and poly(methyl methacrylate) (PMMA) because various two-phase structure having a size of
46 micrometer scale can be obtained at different blend composition; e.g., spherical domain structure is
47 obtained at 30/70 composition while co-continuous structure is obtained at 50/50 composition. Hence,
48 various structural evolution by simultaneous biaxial stretching can be observed by the microscopic
49 observation. The result of the surface hardness estimated by the pencil hardness test was also
50 presented to discuss the structure change by stretching.

51 2. Materials and Methods

52 The PC and PMMA specimens used in this study were commercial polymers. The PC was
53 bisphenol-A polycarbonate supplied by Mitsubishi Gas Chemical Company, Inc; Iupilon S-2000N,
54 $M_w = 2.4 \times 10^4 \text{ g mol}^{-1}$. PMMA was supplied by Kuraray Co., Ltd; Parapet G, $M_w = 1.0 \times 10^5 \text{ g mol}^{-1}$.

55 PC and PMMA were melt-mixed at temperature of 250 °C and at rotor speed of 90 rpm for 5min
56 in a mixing chamber of a miniature mixing machine (Imoto IMC-18D7). The melt mixed blend was
57 extruded and chopped into pellets. The pellets were then melt pressed in a vacuum hot-press
58 machine (Imoto IMC-11FD) at 250 °C and 10 MPa for 5 min to obtain the unstretched film with a
59 thickness of about 100 μm and then was cooled to room temperature. The unstretched film was cut
60 into square-shaped specimen of 65 mm \times 65 mm to employ the biaxial stretching.

61 Biaxial stretching was performed by a biaxial stretcher equipped with a temperature controller
62 (IMC-1A94, Imoto Machinery Co., Ltd.). The film specimen was gripped on each side by 2 pairs of 5
63 clamps (Figure 1) and the initial gauge area before stretching was 50 mm \times 50 mm. Then the specimen
64 was heated to 140 - 160 °C, which was about 10 °C higher than the glass transition temperature of the
65 blends. After keeping the heating temperature for 5 min, the specimen was biaxially stretched to
66 various draw ratios at a draw speed of 100 mm min^{-1} by moving the clamps simultaneously in two
67 stretching directions (X and Y directions as shown by arrows in Figure 1) at the same speed and to
68 the same draw ratio. Then the stretched specimen was cooled to room temperature for the
69 observation.



70 **Figure 1.** Photograph of clamps in a biaxial stretcher.

71

72 Phase structure of the blends was observed under unpolarized optical microscope and also a
73 polarized optical microscope (Olympus BX53-P) equipped with charge-coupled device (CCD) camera
74 (Olympus DP73). The structure under polarized optical microscope was observed by the optical
75 microscope equipped with a sensitive tint plate having an optical path difference of 530 nm under
76 crossed polarizers P and A. Here, the optical axis of polarizer was rotated at 45° to the stretching
77 directions of X and Y, and that of the sensitive tint plate (ST).

78 The phase structure of the blend was also observed under a scanning electron microscope (SEM)
79 (Hitachi S2100A) with an accelerating voltage of 20 kV. In order to observe the surface and cross
80 section of the blend specimen, the PMMA component was etched by 2-butanone for 3 h at room
81 temperature, and the PC one was etched by sodium hydroxide (NaOH) solution (30wt% NaOH) for
82 48 h. For SEM observation, the etched specimen was sputter coated with platinum using a sputter
83 system (JEOL JFC-1300).

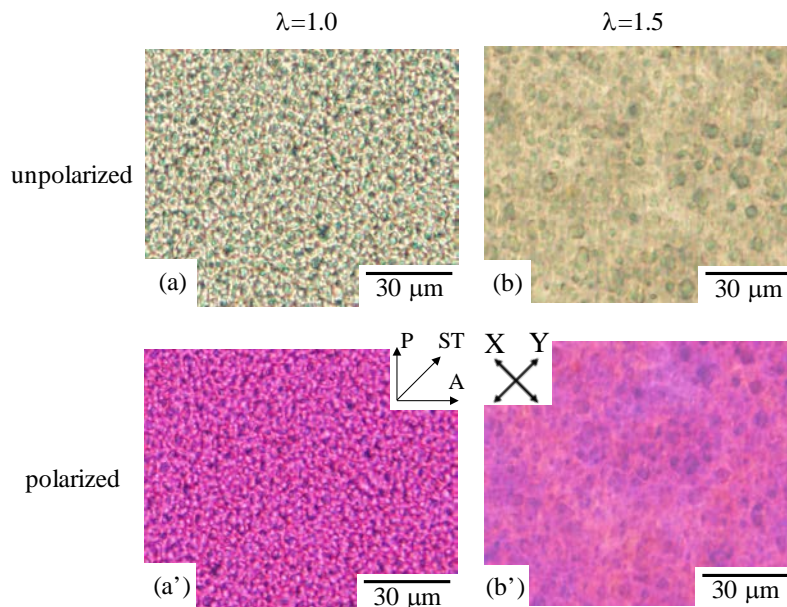
84 The surface hardness of the blend specimen was estimated by pencil hardness test according
85 to ISO 15184. A graphite pencil was drawn on the film specimen with uniform pressure and
86 maintaining the pencil at a constant angle of 45°. The surface hardness was determined using
87 pencils of various degrees of hardness by judging whether indentation was caused or not; i.e., the
88 specimen was judged as harder than pencil hardness when no indentation was seen.

89 3. Results and Discussion

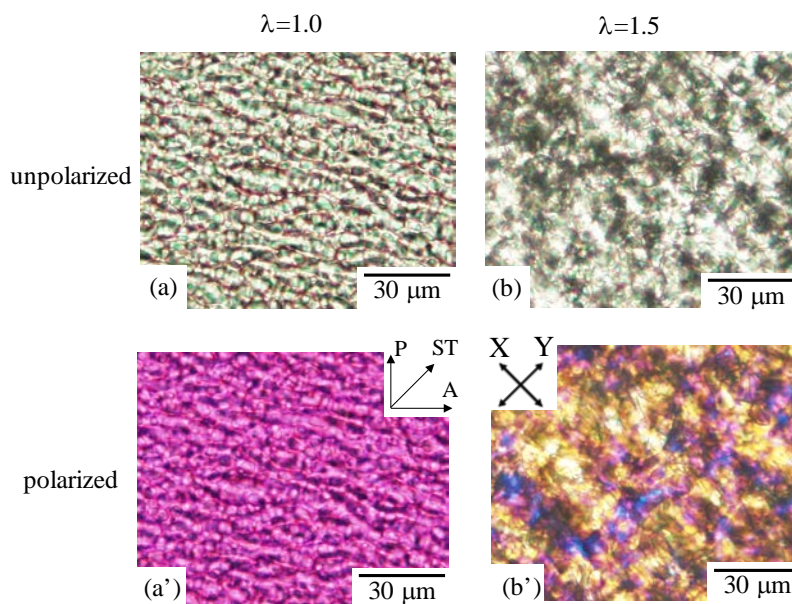
90 Figure 2 shows unpolarized and polarized optical micrographs of 30/70 polycarbonate
91 (PC)/poly(methyl methacrylate) (PMMA) obtained by simultaneous biaxial stretching at draw ratio
92 λ of 1.5 ($\lambda = 1.5$) and the unstretched blend ($\lambda = 1.0$). Spherical PC domains with diameter of several
93 micrometers were dispersed in the PMMA matrix at $\lambda = 1.0$ (Figure 2a). The spherical domain became
94 larger without change of the shape and the domain distance became longer by simultaneous biaxial
95 stretching (Figure 2b), indicating that the two-phase structure of the spherical domain and matrix is
96 enlarged uniformly at all in-plane direction. In spite of the enlargement of the two-phase structure,
97 change of the interference color was small by stretching (Figure 2b'), indicating that the deformed
98 structure was optically isotropic in spite of the stretching. These results suggest that the two-phase
99 structure of the spherical domain and matrix is elongated uniformly at all in-plane direction without
100 preferred orientation by simultaneous biaxial stretching. The results are consistent with those
101 demonstrated in neat polymers such as polypropylene, poly(lactic acid) and poly(ethylene
102 terephthalate) in which the stretched specimen exhibits optically isotropic due to uniform
103 deformation without preferred in-plane orientation by simultaneous biaxial stretching [19,29,31].

104 Co-continuous two-phase structure was obtained in 50/50 PC/PMMA. The change of the co-
105 continuous two-phase structure by simultaneous biaxial stretching is shown in Figure 3. The size of
106 the co-continuous structure became larger by stretching (Figures 3a and 3b). The interesting result
107 here is that blue and yellow interference color appeared, and crosshatched pattern was seen in the
108 stretched blend under the polarized optical microscopy (Figure 3b'), indicating that the component
109 phase is optically anisotropic and the anisotropic-shaped phase is formed along the crosshatched
110 structure. The change and enlargement of the phase structure might be attributed to the evolution of
111 the liquid-liquid phase separation as discussed later in the results of 70/30 PC/PMMA. Blue and
112 yellow interference colors were seen along the crosshatched structure which was elongated to X and

113 Y stretching directions. These results suggest that anisotropic-shaped domain is deformed to X and
 114 Y stretching directions by in-plane bimodal orientation to yield crosshatched structure.



115 **Figure 2.** Unpolarized and polarized optical micrographs of 30/70 PC/PMMA obtained by simultaneous biaxial stretching
 116 at draw ratios λ of 1.0 and 1.5.

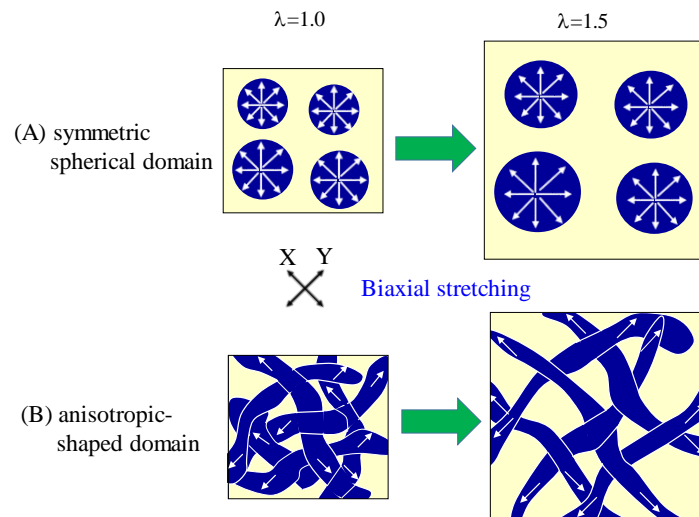


117 **Figure 3.** Unpolarized and polarized optical micrographs of 50/50 PC/PMMA obtained by simultaneous biaxial
 118 stretching at draw ratios λ of 1.0 and 1.5.

119

120 Figure 4 shows the schematic illustration for the deformation of two-phase structure of
 121 PC/PMMA blends by simultaneous biaxial stretching. The symmetric spherical domain is deformed
 122 uniformly at all in-plane direction without preferred orientation by stretching (Figure 4A). On the
 123 other hand, co-continuous two-phase structure consist of unsymmetric anisotropic-shaped domain
 124 and long axis of the anisotropic shaped domain is rotated to X and Y stretching directions, and the
 125 domains are deformed by in-plane bimodal orientation (Figure 4B).

126



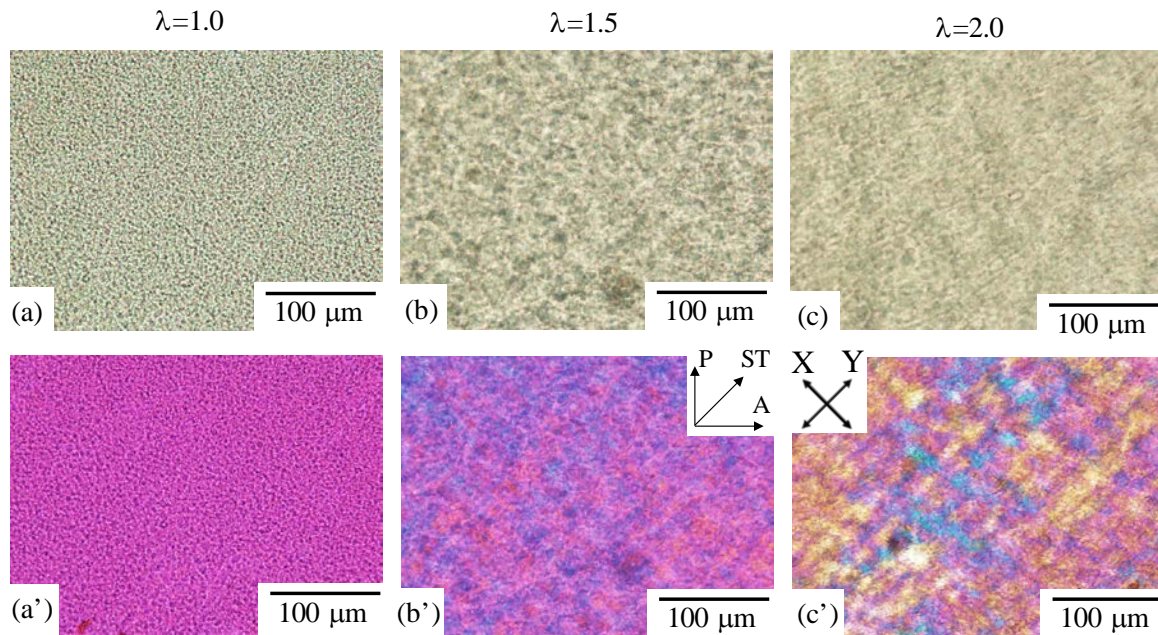
127 **Figure 4.** Schematic illustration for the deformation direction of two-phase structure by simultaneous biaxial
 128 stretching.

129

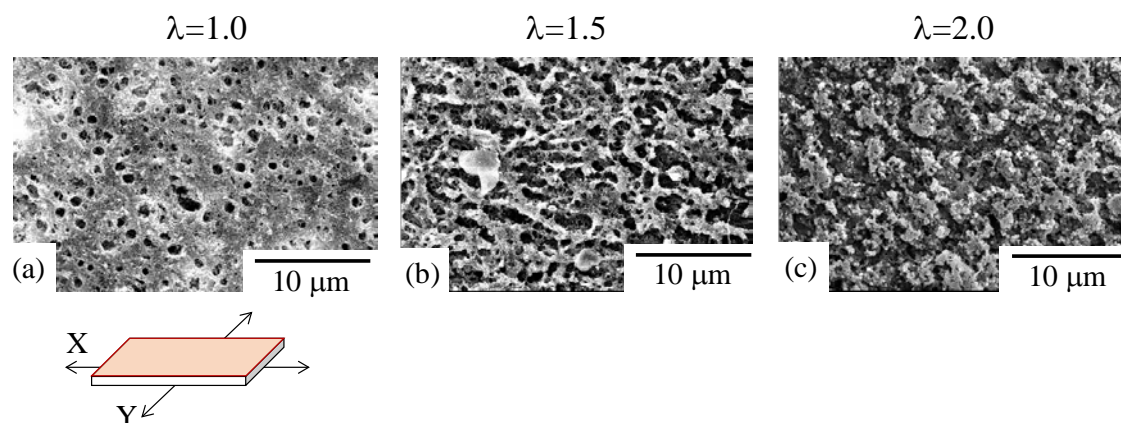
130 In 70/30 PC/PMMA, characteristic change of the two-phase structure occurred as shown in
 131 Figure 5. Two-phase structure of PMMA spherical domains dispersed in the PC matrix was seen in
 132 the unstretched blend (Figure 5a). Though the phase structure with spherical domains was similar to
 133 that observed in Figure 2 for 30/70 PC/PMMA, the structural evolution by stretching was quite
 134 different in 70/30 PC/PMMA. Spherical shape of the PMMA domains changed to the anisotropic-
 135 shaped one (Figures 5b and 5c). Blue and yellow interference color appeared, and crosshatched
 136 pattern was seen under the polarized optical microscopy (Figures 5b' and 5c'), indicating that the
 137 component phase is optically anisotropic and the anisotropic-shaped phase is formed along the
 138 crosshatched structure, though deformed structure was optically isotropic and no change of the
 139 spherical shape was seen in 30/70 PC/PMMA. The change and enlargement of the phase structure
 140 observed in 70/30 PC/PMMA might be attributed to the evolution of the liquid-liquid phase
 141 separation. Crosshatched structure consisting of long fibrils with different interference colors was
 142 observed at $\lambda = 2.0$. Blue and yellow interference color was seen along the crosshatched structure
 143 which was elongated to X and Y stretching directions (Figure 5c'), as observed in Figure 3 for 50/50
 144 PC/PMMA. The interference color for the fibrillar structure aligned in Y direction was yellow.
 145 Considering that the optical axis of sensitive tint plate (ST) is parallel to Y direction, yellow is a
 146 subtractive interference color caused by a component polymer of the blends having a negative
 147 birefringence [35]. Since PMMA has negative birefringence by orientation while PC has positive one
 148 [36], PMMA domain was deformed uniaxially to X and Y stretching direction with in-plane bimodal
 149 deformation to yield crosshatched structure by simultaneous biaxial stretching.

150 Figure 6 shows SEM micrographs of the surface of 70/30 PC/PMMA obtained by simultaneous
 151 biaxial stretching which correspond to the optical micrographs shown in Figure 5. Since SEM
 152 observation was carried out after extraction of PMMA phase by etching with 2-butanone, the
 153 remaining material was PC. Thus spherical holes with diameter of several micrometers seen in Figure
 154 6a are assigned to PMMA domain while white matrix is assigned to PC matrix. This indicates that
 155 PMMA domain is dispersed in PC matrix in the unstretched blend. Spherical domain of PMMA

156 changed to ellipsoidal or fibrillar one, and the aspect ratio increased to X and Y direction with
 157 increasing draw ratio (Figure 6b). This result supports the result demonstrated in Figure 5 that
 158 spherical PMMA domains are elongated to X and Y stretching directions by bimodal in-plane
 159 orientation. At $\lambda = 2.0$, crosshatched network structure was formed in PMMA phase (Figure 6c). That
 160 is, phase inversion occurred by simultaneous biaxial stretching; i.e., PMMA spherical domain was
 161 inverted to the crosshatched network matrix. To our knowledge, this is the first study to observe the
 162 phase inversion by two-phase polymer blends. The phase inversion might be caused by the
 163 coalescence and aggregation of PMMA domains owing to the Ostwald ripening [37] due to evolution
 164 of the liquid-liquid phase separation by stretching, as demonstrated in the following.



165 **Figure 5.** Unpolarized and polarized optical micrographs of 70/30 PC/PMMA obtained by simultaneous biaxial
 166 stretching at various draw ratios λ . Uppers are optical micrographs and lowers are polarized optical micrographs.

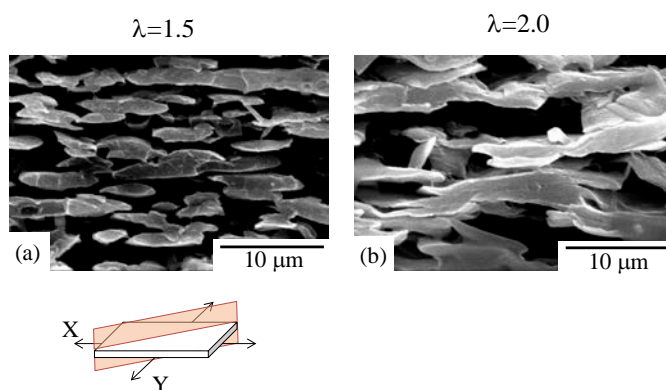


167 **Figure 6.** SEM micrographs of the surface of 70/30 PC/PMMA obtained by simultaneous biaxial stretching at
 168 various draw ratios λ .

169

170 Figure 7 shows SEM micrographs of the cross section of 70/30 PC/PMMA. Since SEM
 171 observation was carried out after extraction of PC phase by etching with NaOH, the remaining
 172 material was PMMA. Spherical domain of PMMA changed to ellipsoidal or fibrillar one in which the

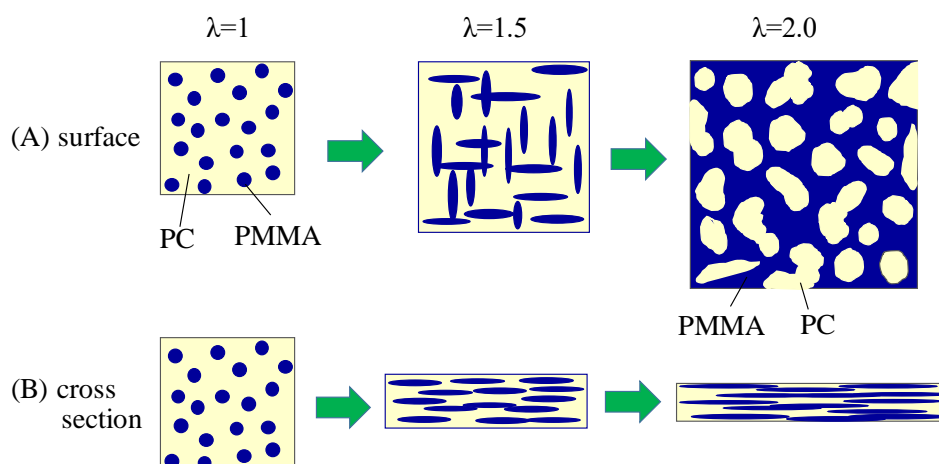
173 major axis of domain is parallel to the plane of films by stretching (Figure 7a). This is consistent with
 174 the in-plane orientation and stretch-thinning in the normal thickness direction suggested in the
 175 simultaneously biaxial stretched films [19,29,31]. PMMA domains were then aggregated in the
 176 thickness direction and the elongated domains became thicker in the thickness direction by the biaxial
 177 stretching (Figure 7b). These results suggest that coalescence and aggregation of PMMA domains
 178 occurred by simultaneously biaxial stretching. Thus phase inversion from PMMA domain to PMMA
 179 matrix by simultaneous biaxial stretching demonstrated in Figure 6 is attributed to the coalescence
 180 and aggregation of PMMA domains. Such coalescence and aggregation of PMMA domains might be
 181 caused by the Ostwald ripening [37] due to evolution of the liquid-liquid phase separation by
 182 stretching.



183 **Figure 7.** SEM micrographs of the cross section of 70/30 PC/PMMA obtained by simultaneous biaxial stretching
 184 at draw ratios λ of 1.5 and 2.0.

185

186 Figure 8 shows the schematic illustration for the structural evolution of 70/30 PC/PMMA
 187 during simultaneously biaxial stretching. Spherical PMMA domains dispersed in the PC matrix are
 188 deformed to ellipsoidal one in X and Y stretching directions. The ellipsoidal domains are coalesced
 189 and aggregated by the Ostwald ripening due to the evolution of the liquid-liquid phase separation.
 190 Owing to the aggregation of the ellipsoidal PMMA domains, long fibrillar PMMA domains are
 191 formed in the X and Y stretching directions by bimodal in-plane orientation. Simultaneously, PMMA
 192 domain is rotated in the in-plane projection and is squashed in the thickness direction by stretch-
 193 thinning. Due to the aggregation of the biaxially deformed PMMA domains, PMMA domains are
 194 inverted to crosshatched matrix.

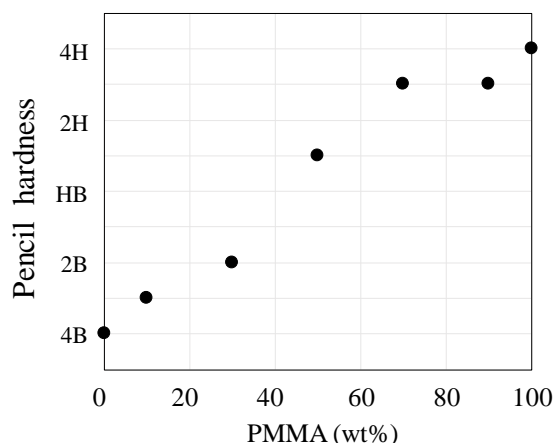


195 **Figure 8.** Schematic illustration for the structure change of 70/30 PC/PMMA by simultaneous biaxial stretching.

196

197

198 Figure 9 shows the surface hardness of the unstretched PC/PMMA films at various blend
 199 compositions. Here the surface hardness was estimated by the pencil hardness test. The surface
 200 hardness of neat PC and neat PMMA was 4B and 4H, respectively. As shown in Figures 2 and 5, the
 201 matrix in 30/70 PC/PMMA and 70/30 PC/PMMA was PMMA and PC, respectively. Hence, the surface
 202 hardness of the blends became harder by increasing the amount of PMMA at the surface with the
 increase of the composition of PMMA.



203

Figure 9. Surface hardness of unstretched PC/PMMA blends at various compositions.

204

205

206

207

208

209

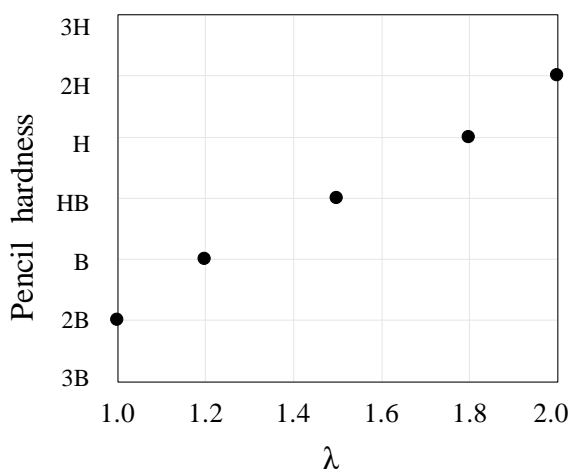
210

211

212

213

Figure 10 shows the surface hardness of 70/30 PC/PMMA film obtained by simultaneous
 biaxial stretching at various draw ratios. The surface hardness became harder with increasing draw
 ratio, e.g., the pencil hardness was 2B at $\lambda = 1.0$, HB at $\lambda = 1.5$ and 2H at $\lambda = 2.0$. By combining the
 results of Figure 9, the surface hardness of the blend at $\lambda = 1.5$ and $\lambda = 2.0$ was close to that of 50/50
 PC/PMMA and 30/70 PC/PMMA, respectively. The change of the surface hardness in 70/30
 PC/PMMA by biaxial stretching is attributed to the increase of the amount of PMMA at the surface
 by structure change from the PMMA domain dispersed in the PC matrix to the PC domain dispersed
 in the PMMA matrix during the stretching. This result confirms the phase inversion of the blend by
 simultaneous biaxial stretching demonstrated in Figures 5-8.



214

Figure 10. Surface hardness of 70/30 PC/PMMA obtained by simultaneous biaxial stretching at various draw ratios λ .

215

216

217 **5. Conclusions**

218 We found characteristic structural evolution in the two-phase blends of polycarbonate (PC)
219 and poly(methyl methacrylate) (PMMA) by simultaneous biaxial stretching. The phase structure
220 was enlarged at all directions without preferred deformation when the symmetric spherical PC
221 domains were dispersed in the PMMA matrix in 30/70 PC/PMMA, while anisotropic-shaped co-
222 continuous structure was deformed to yield crosshatched one in 50/50 PC/PMMA. On the other
223 hand, in 70/30 PC/PMMA, the phase inversion occurred from the spherical PMMA domains to the
224 crosshatched PMMA network matrix by in-plane bimodal orientation due to coalescence and
225 aggregation of the PMMA domains during the biaxial stretching. Owing to the phase inversion,
226 the pencil hardness became harder from 2B to 2H due to the increase of the amount of PMMA at
227 the film surface by the simultaneous biaxial stretching.

228

229 **Acknowledgments:** This work was partially supported by the Japan Society for the Promotion of
230 Science (Grant-in-Aid for Scientific Research (C), No. 18K05231).

231 **Conflicts of Interest:** The authors declare no conflict of interest.

232 **References**

- 233 1. *Biaxial stretching of film: Principles and applications*. Woodhead Publishing: Oxford, 2011.
- 234 2. De Vries, A.; Bonnebat, C.; Beutemps, J. Uni- and biaxial orientation of polymer films and sheets. *J.*
235 *Polym. Sci.: Polym. Symp.* **1977**, *58*, 109-156.
- 236 3. Mascia, L.; Fekkai, Z.; Guerra, G.; Parravicini, L.; Auriemma, F. Effects of distortional components in
237 biaxial stretching of poly(ethylene terephthalate) sheets on dimensional stability and structure. *J. Mat.*
238 *Sci.* **1994**, *29*, 3151-3160.
- 239 4. Kim, J.; Cakmak, M.; Zhou, X. Effect of composition on orientation, optical and mechanical properties
240 of bi-axially drawn PEN and PEN/PEI blend films. *Polymer* **1998**, *39*, 4225-4234.
- 241 5. Cole, K.; Daly, H.B.; Sanschagrin, B.; Nguyen, K.; Aji, A. A new approach to the characterization of
242 molecular orientation in uniaxially and biaxially oriented samples of poly (ethylene terephthalate).
243 *Polymer* **1999**, *40*, 3505-3513.
- 244 6. Elias, M.; Machado, R.; Canevarolo, S. Thermal and dynamic-mechanical characterization of uni- and
245 biaxially oriented polypropylene films. *J. Therm. Anal. Calorim.* **2000**, *59*, 143-155.
- 246 7. Lepersa, J.-C.; Favisa, B.D.; Kent, S.L. Interface-property relationships in biaxially stretched PP-PET
247 blends. *Polymer* **2000**, *41*, 1937-1946.
- 248 8. Dinelli, F.; Assender, H.E.; Kirov, K.; Kolosov, O.V. Surface morphology and crystallinity of biaxially
249 stretched pet films on the nanoscale. *Polymer* **2000**, *41*, 4285-4289.
- 250 9. Marco, Y.; Chevalier, L.; Chaouche, M. Waxd study of induced crystallization and orientation in
251 poly(ethylene terephthalate) during biaxial elongation. *Polymer* **2002**, *43*, 6569-6574.
- 252 10. Douillard, A.; Hardy, L.; Stevenson, I.; Boiteux, G.; Seytre, G.; Kazmierczak, T.; Galeski, A. Texture and
253 morphology of biaxially stretched poly(ethylene naphthalene-2,6-dicarboxylate). *J. Appl. Polym. Sci.*
254 **2003**, *89*, 2224-2232.
- 255 11. Bur, A.J.; Roth, S.C. Real-time monitoring of fluorescence anisotropy and temperature during
256 processing of biaxially stretched polypropylene film. *Polym. Eng. Sci.* **2004**, *44*, 805-813.

- 257 12. Cole, K.C.; Depecker, C.; Jutigny, M.; Lefebvre, J.-M.; Krawczak, P. Biaxial deformation of polyamide-
258 6: Assessment of orientation by means of infrared trichroism. *Polym. Eng. Sci.* **2004**, *44*, 231-240.
- 259 13. Li, Y.; Kaito, A.; Horiuchi, S. Biaxially oriented lamellar morphology formed by the confined
260 crystallization of poly(1,4-butylene succinate) in the oriented blend with poly(vinylidene fluoride).
261 *Macromolecules* **2004**, *37*, 2119-2127.
- 262 14. Nie, H.Y.; Walzak, M.J.; McIntyre, N.S. Atomic force microscopy study of biaxially oriented
263 polypropylene films. *J. Mater. Eng. Perform.* **2004**, *13*, 451-460.
- 264 15. Ajjji, A.; Zhang, X.; Elkoun, S. Biaxial orientation in hdpe films: Comparison of infrared spectroscopy,
265 x-ray pole figures and birefringence techniques. *Polymer* **2005**, *46*, 3838-3846.
- 266 16. Li, Y.; Oono, Y.; Nakayama, K.; Shimizu, H.; Inoue, T. Dual lamellar crystal structure in poly(vinylidene
267 fluoride)/acrylic rubber blends and its biaxial orientation behavior. *Polymer* **2006**, *47*, 3946-3953.
- 268 17. Je'ol, S.p.; Fenouillot, F.; Rousseau, A.; Masenelli-Varlot, K.; Gauthier, C.; Briois, J.-F. Drastic
269 modification of the dispersion state of submicron silica during biaxial deformation of poly(ethylene
270 terephthalate). *Macromolecules* **2007**, *40*, 3229-3237.
- 271 18. Chapleau, N.; Huneault, M.A.; Li, H. Biaxial orientation of polylactide/thermoplastic starch blends. *Int.*
272 *Polym. Process.* **2007**, *22*, 402-409.
- 273 19. Ou, X.; Cakmak, M. Influence of biaxial stretching mode on the crystalline texture in polylactic acid
274 films. *Polymer* **2008**, *49*, 5344-5352.
- 275 20. Sweeney, J.; Spares, R.; Woodhead, M. A constitutive model for large multiaxial deformations of solid
276 polypropylene at high temperature. *Polym. Eng. Sci.* **2009**, *49*, 1902-1908.
- 277 21. X. Ou, M.C. Comparative study on development of structural hierarchy in constrained annealed
278 simultaneous and sequential biaxially stretched polylactic acid films. *Polymer* **2010**, *51*, 783-792.
- 279 22. Abu-Zurayk, R.; Harkin-Jones, E.; McNally, T.; Menary, G.; Martin, P.; Armstrong, C.; McAfee, M.
280 Structure-property relationships in biaxially deformed polypropylene nanocomposites. *Composites*
281 *Science and Technology* **2010**, *70*, 1353-1359.
- 282 23. Yoshida, S.; Ishii, K.; Kawamura, T.; Nitta, K.-H. Molecular orientation behavior of mesomorphic
283 isotactic polypropylene under uniaxial and biaxial deformation. *Polym. Eng. Sci.* **2011**, *51*, 225-231.
- 284 24. Yoshida, S.; Sawada, T.; Kawamura, T.; Nitta, K.-h. Investigation of a rheo-optical method for
285 determining the in-situ molecular orientation behavior in stretching films under biaxial deformation.
286 *Polym. Test.* **2011**, *30*, 893-898.
- 287 25. Buckley, C.P.; Lew, C.Y. Biaxial hot-drawing of poly(ethylene terephthalate): An experimental study
288 spanning the processing range. *Polymer* **2011**, *52*, 1803-1810.
- 289 26. Tsunekawa, T.; Higashioji, T.; Hosokawa, H.; Kubota, A.; Ishizuka, I. Development and
290 industrialization of a biaxially stretched nano-alloyed film. *Polym. J.* **2012**, *44*, 1170-1178.
- 291 27. Tamura, S.; Kuramoto, I.; Kanai, T. The effect of molecular structure of polypropylene on stretchability
292 for biaxially oriented film. *Polym. Eng. Sci.* **2012**, *52*, 1383-1393.
- 293 28. Tabatabaei, S.H.; Ajjji, A. Crystal structure and orientation of uniaxially and biaxially oriented pla and
294 pp nanoclay composite films. *J. Appl. Polym. Sci.* **2012**, *124*, 4854-4863.
- 295 29. Hassan, M.; Cakmak, M. Mechano optical behavior of polyethylene terephthalate films during
296 simultaneous biaxial stretching: Real time measurements with an instrumented system. *Polymer* **2013**,
297 *54*, 6463-6470.
- 298 30. Hassan, M.K.; Cakmak, M. Mechanisms of structural organizational processes as revealed by real time
299 mechano optical behavior of pet film during sequential biaxial stretching. *Polymer* **2014**, *55*, 5245-5254.

- 300 31. Al-Itry, R.; Lamnawar, K.; Maazouz, A.; Billon, N.; Combeaud, C. Effect of the simultaneous biaxial
301 stretching on the structural and mechanical properties of pla, pbat and their blends at rubbery state.
302 *Eur. Polym. J.* **2015**, *68*, 288-301.
- 303 32. Jariyasakoolroj, P.; Tashiro, K.; Wang, H.; Yamamoto, H.; Chinsirikul, W.; Kerddonfag, N.;
304 Chirachanchai, S. Isotropically small crystalline lamellae induced by high biaxial-stretching rate as a
305 key microstructure for super-tough polylactide film. *Polymer* **2015**, *68*, 234-245.
- 306 33. Nitta, K.-h.; Sawada, T.; Yoshida, S.; Kawamura, T. Three dimensional molecular orientation of isotactic
307 polypropylene films under biaxial deformation at higher temperatures. *Polymer* **2015**, *74*, 30-37.
- 308 34. Feng, J.; Zhang, G.; MacInnis, K.; Olah, A.; Baer, E. Formation of microporous membranes by biaxial
309 orientation of compatibilized PP/nylon 6 blends. *Polymer* **2017**, *123*, 301-310.
- 310 35. Sawyer, L.; Grubb, D.T.; Meyers, G.F. *Polymer microscopy*. Springer Science & Business Media: 2008.
- 311 36. Saito, H.; Inoue, T. Chain orientation and intrinsic anisotropy in birefringence-free polymer blends. *J.*
312 *Polym. Sci., Part B: Polym. Phys.* **1987**, *25*, 1629-1636.
- 313 37. Ratke, L.; Voorhees, P.W. *Growth and coarsening: Ostwald ripening in material processing*. Springer: Berlin,
314 2002.
- 315